CROATICA CHEMICA ACTA CCACAA **75** (3) 663–681 (2002)

ISSN-0011-1643
CCA-2824 *Original Scientific Paper*

Kinetic Analysis of Crystal Growth of Zeolite A

*Sanja Bosnar and Boris Subotić**

Ruđer Bošković Intitute, Laboratory for the Synthesis of New Materials, Division of Material Chemistry, P.O. Box 180, Zagreb, Croatia

Received September 26, 2001; revised May 15, 2002; accepted May 16, 2002

Changes of the concentrations of aluminium, c_{Al}, and of silicon, c_{Si}, in the liquid phase as well as of the dimension, L_m, of the largest crystals were measured during crystallization of zeolite A from the amorphous aluminosilicate precursor ($1.03\ Na_2O \cdot Al_2O_3 \cdot 2.38\ SiO_2 \cdot 1.66\ H_2O$) dispersed in alkaline solutions (1.2 or 1.4 M NaOH solution) containing or not containing dissolved Al_2O_3 and/or SiO_2 of appropriate concentrations. Analysis of the relationship between the concentration factors $f(c) = f(c_{Al}, c_{Si})$ relevant to different growth models and the growth rate of zeolite A crystals have shown that the growth is governed by the reaction of monomeric and/or low-molecular aluminate, silicate and aluminosilicate anions from the liquid phase on the surfaces of growing zeolite crystals, and hence that the kinetics of the growth rate of zeolite A crystals may be expressed as: $dL/dt_c = k_g [c_{Al} - c_{Al}(eq)][c_{Si} - c_{Si}(eq)] = k_g f(c)$, where t_c is the time of crystallization, $c_{Al}(eq)$ and $c_{Si}(eq)$ are the aluminium and silicon concentrations in the liquid phase, corresponding to the solubility of zeolite A under given crystallization conditions, and k_g is the rate constant of the linear growth of zeolite A crystals.

Key words: zeolite A, crystallization, crystal growth, mechanism, kinetics.

INTRODUCTION

The crystal growth rate of solids, including zeolites, from supersaturated solutions is commonly expressed as a function of the concentration(s),

* Author to whom correspondence should be addressed. (E-mail: subotic@rudjer.irb.hr)

$f(c)$, of ions or molecules in solution,[1–4] *i.e.*,

$$\mathrm{d}L/\mathrm{d}t_c = k_g f(c) \tag{1}$$

where k_g is the growth rate constant. The growth rate may be controlled by the rate of transport of ions or molecules from the liquid phase to the surfaces of the growing crystals, the rate of the reaction of ions or molecules from the liquid phase on the surfaces of the growing crystals, and/or the rate of incorporation of ions or molecules into crystals.[5–7]

When transport of ions or molecules from the liquid phase to the surfaces of the growing crystals is controlled by their diffusion through the concentration gradient formed around the growing crystals (unstirred systems), the growth rate, $R = \mathrm{d}r/\mathrm{d}t$, of spherical particles having radius r, is directly proportional to the absolute supersaturation, $f(c)_1 = c - c(\mathrm{eq})$, and inversely proportional to the particle (crystal) size r,[1,6] *i.e.*,

$$\mathrm{d}r/\mathrm{d}t = DV_m[c - c(\mathrm{eq})]/r = k_g(1)[c - c(\mathrm{eq})]/r = k_g(1)\, f(c)_1/r \tag{2}$$

where D is the diffusion coefficient of reactive ions or molecules in the solution, V_m is their ionic (molecular) volume, c is the concentration of the reactive ions or molecules in the solution (the salt solution concentration), $c(\mathrm{eq})$ is the salt solubility, and $k_g(1) = DV_m$.

When the concentration gradient around the growing particles is disturbed (*i.e.*, during sedimentation in the gravitation and/or centrifugal field, or in stirring), the diffusion-controlled crystal growth may be expressed as:

$$\mathrm{d}r/\mathrm{d}t = DV_m[c - c(\mathrm{eq})]/\delta \tag{3}$$

where δ is the thickness of the stationary diffusion layer (hydrodynamic boundary layer) around the growing particles, determined by the particle size, viscosity of the solution, difference between the densities of the solid and the liquid phases and the relative speed of particles.[6]

When the system is vigorously stirred, the concentration gradient around the growing particles may be reduced to a negligible value, and then the rate of crystal growth is controlled by the rate of transport (*e.g.*, convection) of ions or molecules from the liquid phase to the surfaces of the growing crystals, *i.e.*,

$$\mathrm{d}r/\mathrm{d}t = k_g(2)[c - c(\mathrm{eq})] = k_g(2)\, f(c)_1 \tag{4}$$

where $k_g(2)$ is a constant determined by the difference between the densities of the solid and the liquid phases, and the rate of motion of the solution, but not by the diffusion coefficient of the reactive ions or molecules. Equation (4) has been widely used to interpret and predict the crystal growth rate of many solids,[8–10] including zeolites.[11–14]

Equations (4) to (6) are valid for simple monomolecular compounds,[1] but the diffusion-controlled growth of electrolytes of the AB type, or double salts, is described by a more complex equation,[1] *i.e.*,

$$\mathrm{d}r/\mathrm{d}t = DV_m\{c_A + c_B - [(c_A - c_B)^2 + 4K_{sp}]^{1/2}\}/2r =$$

$$= k_g(3)\{c_A + c_B - [(c_A - c_B)^2 + 4K_{sp}]^{1/2}\}/r = k_g(3)\, f(c)_2/r \qquad (5)$$

where $D = D_A$ (diffusion coefficients of ion A) $\approx D_B$ (diffusion coefficients of ion B), K_{sp} is the solubility product, $k_g(3) = DV_m/2$ and $f(c)_2 = \{c_A + c_B - [(c_A - c_B)^2 + 4K_{sp}]^{1/2}\}$.

Finally, the equation,

$$\mathrm{d}L/\mathrm{d}t = k[c - c(\mathrm{eq})]^n \qquad (6)$$

has been frequently used to describe the rate of surface-reaction-controlled crystal growth of the A_aB_b type of solids.[15–18] The relationship between the crystal growth rate, $\mathrm{d}L/\mathrm{d}t$, and the concentration dependence in Eq. (6) may be explained by the Davies and Jones model of dissolution and growth,[15,19] which predicts formation of a monolayer of solvated ions with a constant composition at the surface of the growing/dissolving crystals. According to this model, the rate of crystal growth of a solid A_aB_b is proportional to the product of fluxes of the ions (molecules) participating in the surface reaction, *i.e.*,

$$\mathrm{d}L/\mathrm{d}t = k_3[c_A - c_A(\mathrm{eq})]^a[c_B - c_B(\mathrm{eq})]^b =$$

$$k_3(\mathrm{A})\,(b/a)^{1/b}[c_A - c_A(\mathrm{eq})]^{a+b} = k_3(\mathrm{B})\,(a/b)^{1/a}[c_B - c_B(\mathrm{eq})]^{a+b} =$$

$$k_g(\mathrm{A})[c_A - c_A(\mathrm{eq})]^n = k_g(\mathrm{B})[c_B - c_B(\mathrm{eq})]^n \qquad (7)$$

where $k_g(\mathrm{A}) = k_3(\mathrm{A})\,(b/a)^{1/b}$ and $k_g(\mathrm{B}) = k_3(\mathrm{B})\,(a/b)^{1/a}$ are factors proportional to the growth rate constant k_g, and $n = a + b$.

Although there is abundant evidence that the crystal growth of zeolites is a function of concentrations of both silicon and aluminium in the liquid

phase,[2–4,20–25] the question of the mechanism of the crystal growth of zeolites, and hence of the relationship between the crystal growth rate, dL/dt_c, and the concentrations, of aluminium, c_{Al}, and of silicon, c_{Si}, in the liquid phase is still open.

Hence, our intention is: (i) to analyze the kinetics of the crystal growth of zeolite A crystallized under different conditions according to the different growth models described below, in order to define the mechanism of the crystal growth of zeolite A, and (ii) to find out the relationship between the crystal growth rate and the concentrations of silicon and aluminium in the liquid phase. The kinetic models expressed by Eqs. (2), (4), (5) and (7) are used for the analysis of the kinetics of the crystal growth of zeolite A crystallized under different conditions (see Experimental).

EXPERIMENTAL

Aqueous aluminosilicate gel having the oxide molar composition: 2.97 $Na_2O \cdot Al_2O_3 \cdot 1.93\ SiO_2 \cdot 127.96\ H_2O$ was prepared by pipetting 100 ml of sodium silicate solution of appropriate concentration with respect to Na_2O and SiO_2 into a plastic beaker containing 100 ml of propeller stirred sodium aluminate solution of appropriate concentration with respect to Na_2O and Al_2O_3. Sodium aluminate solution (0.7576 M in Al_2O_3) was prepared by dissolving anhydrous $NaAlO_2$ (41% Na_2O and 54% Al_2O_3; mass fractions, w) in distilled water and sodium silicate solution was prepared by dissolving anhydrous Na_2SiO_3 (51% Na_2O and 48% SiO_2) in distilled water. The solutions were thermostated to 25 °C before being mixed together. The gel prepared as described above was centrifuged to separate the solid from the liquid phase. The clear liquid phase (supernatant) above the sediment (amorphous aluminosilicate precipitated during the gel preparation) was carefully removed without disturbing the solid phase (sediment). After removal of the supernatant, the solid phase was redispersed in distilled water and centrifuged repeatedly. The procedure was repeated until the pH value of the liquid phase above the sediment was 9.

A small part of the washed solid phase was dried overnight at 105 °C and cooled in a desiccator over silicagel. To determine the content of water, part of the sample was weighed and then calcined at 800 °C for 2 h. A certain amount of the calcined (waterless) sample was dissolved in a 1:1 HCl solution. The solution was diluted with distilled water to the concentration ranges suitable for measuring the concentrations of sodium, aluminium and silicon by atomic absorption spectroscopy. The rest of the washed solid phase (amorphous aluminosilicate having the chemical composition: 1.03 $Na_2O \cdot Al_2O_3 \cdot 2.38\ SiO_2 \cdot 1.66\ H_2O$) was redispersed in distilled water, so that the prepared suspension contained 16% (w) of the solid phase. 100 ml of the suspension was poured into a stainless-steel reaction vessel and then warmed up at 80 °C. The reaction vessel was provided with a thermostated jacket and fitted with a water-cooled reflux condenser and thermometer. When the suspension was thermostated at the reaction temperature (80 °C), 100 ml of the solution containing 2.4 mol dm^{-3} NaOH (system I), 2.8 mol dm^{-3} NaOH + 0.034 mol dm^{-3} SiO_2 (system II), and 2.8 mol dm^{-3} NaOH + 0.09 mol dm^{-3} Al_2O_3 (system III) thermostated at 80 °C was

quickly added to the suspension. Thus prepared reaction mixtures contained 8% (w) of the solid phase (1.03 $Na_2O \cdot Al_2O_3 \cdot 2.38\ SiO_2 \cdot 1.66\ H_2O$) dispersed in the appropriate liquid phase. The reaction mixtures were heated at 80 °C under stirring with a Teflon-coated magnetic bar driven by a magnetic stirrer. At various times, t_c, after the beginning of the crystallization process, aliquots of the reaction mixture were drawn off to prepare samples for analysis. The moment when the NaOH solution was added to the previously prepared suspension was taken as zero time of the crystallization process.

Aliquots of the reaction mixture drawn off at given crystallization times, t_c, were poured into cuvettes and centrifuged to stop the crystallization process and to separate the solid from the liquid phase. Part of the clear liquid phase (supernatant) was diluted with distilled water to the concentration ranges suitable for measuring the concentrations of aluminium and silicon by atomic absorption spectroscopy. The rest of the supernatant was carefully removed without disturbing the solid phase (sediment). After removal of the supernatant, the solid phase was redispersed in distilled water and centrifuged repeatedly. The procedure was repeated until the pH value of the liquid phase above the sediment was 9. The wet washed solids were dried overnight at 105 °C, then cooled in a desiccator with silicagel and then pulverized in an agate mortar. The powdered solids were used to determine the fraction of zeolite A, w_{ZA}, and to measure the size of the largest crystals, L_m.

The X-ray spectra of the samples were taken by a Philips diffractometer (Cu-Kα radiation) in the corresponding region of Bragg's angles. The mass fractions of crystalline and amorphous phases were calculated by a mixed method,[26] using the integral value of the broad amorphous peak (2θ = 17–39°) and the corresponding sharp peaks of crystalline phase.

Concentrations of sodium, aluminium and silicon in the solutions obtained by dissolving the calcined samples and in those obtained by the dilution of the liquid phases separated from the reaction mixtures at various crystallization times, t_c, were measured using the Perkin-Elmer 3030B atomic absorption spectrometer.

The size of the largest crystals in the solid samples drawn off the reaction mixture at various crystallization times, t_c, were determined by the method proposed by Zhdanov,[21] using optical microscopy.

RESULTS AND DISCUSSION

Figures 1–3 show changes in the fraction of zeolite A, w_{ZA} (A), concentrations $c = c_{Al}$ and $c = c_{Si}$ (B) as well as the size of the largest crystals of zeolite A, L_m (C), during zeolite A crystallization from the systems I (Figure 1), II (Figure 2) and III (Figure 3). Concentration c_{Al} of aluminium in the liquid phase is approximately constant or decreases slowly during the main part of the crystallization process, then it drops suddenly at the end of the crystallization process and gradually decreases until the equilibrium concentration $c_{Al} = c_{Al}(eq)$ is reached. On the other hand, the concentration c_{Si} of silicon in the liquid phase is approximately constant during the »induction period« of the crystallization process, and then it increases in the course of crystalliza-

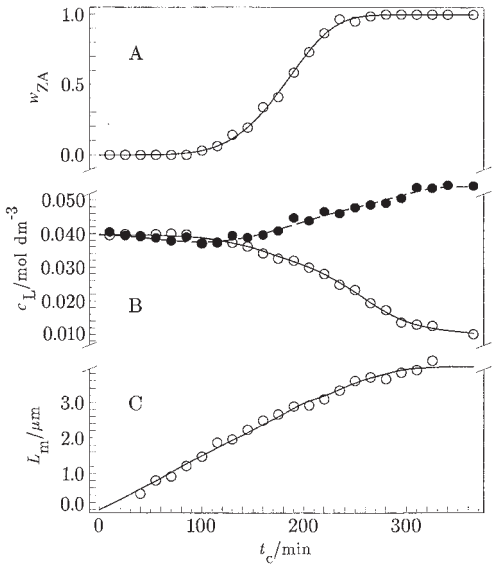

Figure 1. Changes in A) fraction of zeolite A, w_{ZA}; B) concentrations $c_L = c_{Al}$ (○, solid curve) and $c_L = c_{Si}$ (●, dashed curve); and C) size of the largest crystals, L_m, of zeolite A during its crystallization in system I. t_c is the time of crystallization.

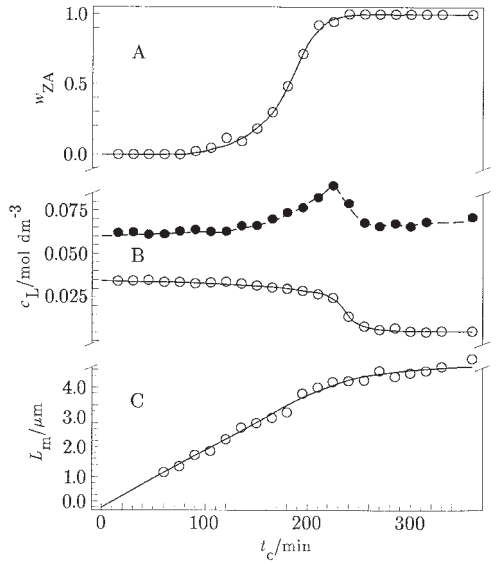

Figure 2. Changes in A) fraction of zeolite A, w_{ZA}; B) concentrations $c_L = c_{Al}$ (○, solid curve) and $c_L = c_{Si}$ (●, dashed curve); and C) size of the largest crystals, L_m, of zeolite A during its crystallization in system II. t_c is the time of crystallization.

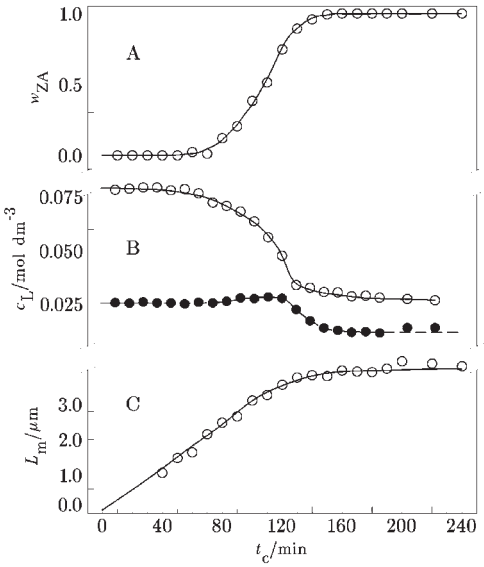

Figure 3. Changes in A) fraction of zeolite A, w_{ZA}; B) concentrations $c_L = c_{Al}$ (○, solid curve) and $c_L = c_{Si}$ (●, dashed curve); and C) size of the largest crystals, L_m, of zeolite A during its crystallization in system III. t_c is the time of crystallization.

tion (system I), or increases during the period of increased crystallization rate, reaches a maximum value at the end of the crystallization process, and then drops suddenly to any constant value (systems II and III). The increase in c_{Si} during the period of increased crystallization rate is caused by the lower Si/Al ratio (Si/Al = 1) in the crystallized zeolite A than in the starting amorphous aluminosilicate precursor (Si/Al = 1.19). Since more than 90% of Si and Al is contained in the solid phase (aluminosilicate precursor), the differences in the change of c_{Si} as well as in the final concentration of silicon in the liquid phase of different systems are probably caused by small variations of the Si/Al ratio in the precursors and the content of the precursor in the systems, respectively.

The linear relationship between the time of crystallization, t_c, and the size, L_m, of the largest zeolite crystals (Figures 1C to 3C) for small variations in $f(c)$ (see Figure 4) indicates that the growth of zeolite crystals is size independent,[21,27–30] *i.e.*, »that not only during the period of constant linear growth rate, but also during the final decay period crystals of all sizes grew at the same but declining linear rate«.[27] Such postulation may be justified by a linear growth of the seed crystal of zeolite Y added to hydrogel[31,32] as well as by the linear growth of monodisperse crystals of different types of zeolites during their crystallization from clear aluminosilicate solutions.[33–44]

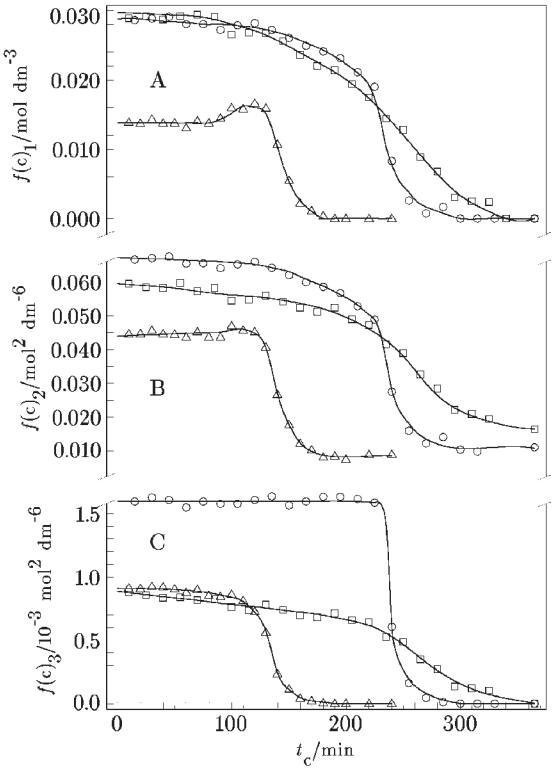

Figure 4. Changes in concentration functions $f(c)_1$ (A), $f(c)_2$ (B), and $f(c)_3$ (C), during crystallization of zeolite A in systems I (□), II (○), and III (Δ). t_c is the time of crystallization.

The same conclusion was drawn on the basis of a direct measurement of the growth rate of zeolite ZSM-5 monocrystals.[45] Based on this postulation, and taking into consideration the chemical composition of zeolites, *i.e.*, $Na_2O \cdot Al_2O_3 \cdot x\,SiO_2 \cdot y\,H_2O$, (the aluminosilicate cage may be formally considered as a compound of AB_b type, where A = Al, B = Si, and $b = x\,SiO_2/Al_2O_3$) integration of Eqs. (2), (4), (5), and (7) from 0 to t_c gives:

$$r^2 = (L_m)^2 = 2k_g(1)\int_0^{t_c}[c_z - c_z(\mathrm{eq})]\mathrm{d}t_c = 2k_g(1)\int_0^{t_c} f(c)_1\mathrm{d}t_c = k_g(1)'I_1 \qquad (8)$$

$$r = L_m = k_g(2)\int_0^{t_c}[c_z - c_z(\mathrm{eq})]\mathrm{d}t_c = k_g(2)\int_0^{t_c} f(c)_1\mathrm{d}t_c = k_g(2)'I_1 \qquad (9)$$

$$r^2 = (L_m)^2 = 2k_g(3)\int_0^{t_c}\{c_{Al} + c_{Si} - [(c_{Al} - c_{Si})^2 + 4c_{Al}(eq)c_{Si}(eq)]^{1/2}dt_c = 2k_g(3)\int_0^{t_c} f(c)_2 dt_c = k_g(3)'I_2 \quad (10)$$

$$L_m = k_g(4)\int_0^{t_c}[c_{Al} - c_{Al}(eq)][c_{Si} - c_{Si}(eq)]^b dt_c = k_g(4)\int_0^{t_c} f(c)_3 dt_c = k_g(4)'I_3 \quad (11)$$

For the systems having an »excess« of silicon in the liquid phase (systems I and II; see Figures 1B and 2B), concentrations c_z (concentration of zeolite dissolved in the liquid phase during crystallization) and $c_z(eq)$ (solubility of zeolite under given synthesis conditions) are determined by the corresponding concentrations of c_{Al} and $c_{Al}(eq)$ (Figures 1–3), and hence $f(c)_1 = [c_{Al} - c_{Al}(eq)]$. For the same reason, for the systems having an »excess« of aluminium in the liquid phase (system III; see Figure 3B), $f(c)_1 = [c_{Si} - c_{Si}(eq)]$. Here, c_{Al} and c_{Si} are concentrations of aluminium and silicon in the liquid phase during crystallization while $c_{Al}(eq)$ and $c_{Si}(eq)$ are concentrations of aluminium and silicon in the liquid phase which correspond to the solubility of zeolite under given crystallization conditions. Hence, $k_g(1)' = 2\ k'k_g(1)$, $k_g(2)' = k'k_g(2)$, and $k_g(3)' = 2\ k_g(3)$, where k' represents the amounts of aluminium or silicon (n_{Al}, n_{Si}) in 1 mole of zeolite (k'= 2 for zeolite A; $Na_2O \cdot Al_2O_3 \cdot 2\,SiO_2 \cdot 4.5H_2O$).

Values of concentration functions $f(c)_1 = c_{Al} - c_{Al}(eq)$ (for systems I and II), $f(c)_1 = c_{Si} - c_{Si}(eq)$ (for system III), $f(c)_2 = c_{Al} + c_{Si} - [(c_{Al} - c_{Si})^2 + 4\ c_{Al}(eq)c_{Si}(eq)]^{1/2}$, and $f(c)_3 = [c_{Al} - c_{Al}(eq)][c_{Si} - c_{Si}(eq)]^b$ (b = 1 for zeolite A) were calculated by the corresponding values of aluminium and silicon concentrations in the liquid phase (Figures 1B–3B), and represented as functions of the crystallization time t_c in Figure 4. Values of integrals

$$I_1 = \int_0^{t_c} f(c)_1 dt_c,\ I_2 = \int_0^{t_c} f(c)_2 dt_c,\ \text{and}\ I_3 = \int_0^{t_c} f(c)_3$$

were calculated by numerical (graphical) integration of the corresponding concentration functions in Figures 4A–4C. Using the values of integrals I_1 (Figure 5A), I_2 (Figure 5B), and I_3 (Figure 5C), relevant to different crystallization times t_c during crystallization of zeolite A in systems I to III, and the corresponding values of L_m (Figures 1C–3C), the values of $k_g(1)'$ in Eq. (8), $k_g(2)'$ in Eq. (9), $k_g(3)'$ in Eq. (10), and $k_g(4)'$ in Eq. (11) were, for different crystallization times t_c, calculated as:

$$k_g(1)' = (L_m)^2 / \int_0^{t_c} f(c)_1 dt_c = (L_m)^2 / I_1 \quad (12)$$

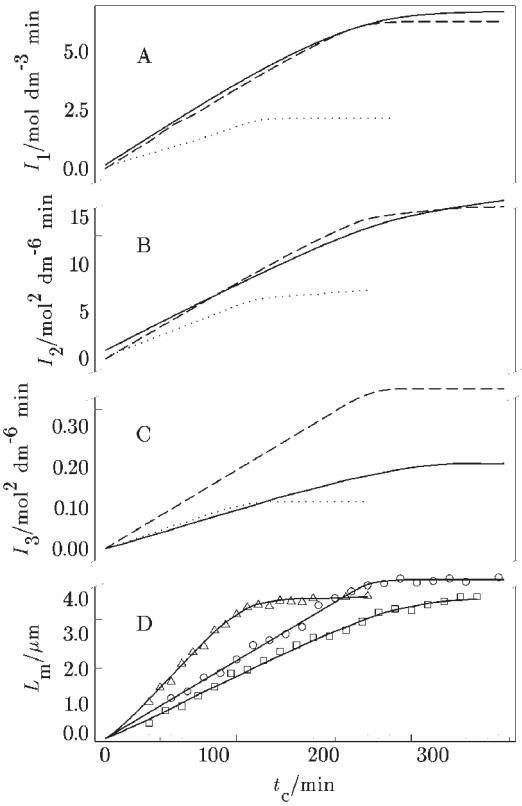

Figure 5. Changes in the values of integrals: I_1 of the concentration function $f(c)_1$ (A); I_2 of the concentration function $f(c)_2$ (B); and I_3 of the concentration function $f(c)_3$ (C); during crystallization of zeolite A in systems I (solid curves), II (dashed curves), and III (dotted curves). Fig. D shows size of the largest crystals, L_m, of zeolite A during its crystallization in systems I (□), II (○) and III (Δ). Curves in Fig. D represent the L_m *vs.* t_c functions calculated by Eq. (16) using the average value of k_g (Table IV) and the corresponding values of I_3 (Fig. 5C)

$$k_g(2)' = L_m / \int_0^{t_c} f(c)_1 \mathrm{d}t_c = L_m / I_1 \tag{13}$$

$$k_g(3)' = (L_m)^2 / \int_0^{t_c} f(c)_2 \mathrm{d}t_c = (L_m)^2 / I_2 \tag{14}$$

$$k_g(4)' = L_m / \int_0^{t_c} f(c)_3 \mathrm{d}t_c = L_m / I_3 \tag{15}$$

Values of $k_g(1)'$, $k_g(2)'$, $k_g(3)'$ and $k_g(4)'$, calculated by Eqs. (12) to (15) for different crystallization times t_c, are listed in Tables I–IV.

Kinetics of crystal growth, described by Eqs. (2), (4), and (5), implicitly include that reactive species (molecules) in the liquid phase, determined by their concentrations c and c(eq), have the same chemical composition and/or structure as the growing crystals of the solid phase. Such reactive species may reach the surface of the growing crystals by diffusion through the concentration gradient (Eq. 2), by diffusion through the hydrodynamic boundary layer (Eq. 3), or by convection (Eq. 4). Some authors assume formation of »structured« aluminosilicate blocks (S-species,[11,46] unit cells[47–51]) in the liquid phase and their transport from the solution onto the surfaces of the growing crystals. Such a model is close to those described by Eqs. (2) to (4) (c is the concentration of »structured« aluminosilicate blocks in the liquid phase during crystallization and c(eq) is the concentration of »structured« aluminosilicate blocks in the liquid phase, which correspond to the solubility of crystallized zeolite), and it assumes a convection controlled and/or diffusion controlled growth. On the other hand, there is no evidence for the existence of complex silicate and aluminosilicate structures in the liquid phase of crystallizing systems. Spectroscopic analyses of the liquid phase during crystallization of different types of zeolites[52–54] have shown that the liquid phase contains $Al(OH)_4^-$ monomers and different low-molecular silicate and aluminosilicate anions. Furthermore, according to Barrer,[27] a growth mechanism governed by diffusional control can be ruled out because of the high activation energy obtained by measuring the linear growth rates of zeolites A (47.3 kJ mol^{-1}),[20] X (62.6 kJ mol^{-1}),[21] Y (49–65 kJ mol^{-1}),[31,32] and silicalite-1 (42 kJ mol^{-1}),[36] whereas a diffusional mechanism would be expected to yield an activation energy of 12–17 kJ mol^{-1}. In this context, variability of the values of $k_g(1)'$, and $k_g(3)'$ (see Tables I and III) was expected. On the other hand, constancy of the $k_g(2)'$ value during a certain period of crystallization (Table II) is caused rather by a linear change of both L_m (see Figures 1C–3C) and I_1 (see Figure 5A) during the same period of crystallization than by the relevance of the convection-controlled transport of reactive silicate and aluminate species to the crystal growth kinetics. Deviations from the constancy of the $k_g(2)'$ values, which coincide with deviations from the linearity of the L_m *vs.* t_c (Figures 1C–3C) and I_1 *vs.* t_c (Figure 5A) functions, corroborate this conclusion. These results indicate that the crystal growth of zeolite A is not controlled by the simple transport of reactive silicate and aluminate species from the liquid phase on the surfaces of growing zeolite crystals (*e.g.*, diffusion or convection; see Eqs. (2), (4), and (5)). On the other hand, constancy of the value of $k_g(4)' = k_g$ during the entire process of zeolite A crystallization under different conditions (see Table IV) strongly indicates that

TABLE I

Dependence of the value of factor $k_g(1)'$ on the crystallization time t_c, during crystallization of zeolite A in systems I, II, and III

t_c/min	$k_g(1)'$/μm^2 min^{-1} mol^{-1} dm^3		
	system I	system II	system III
10	–	–	0.40
15	–	0.17	–
20	0.12	–	0.95
30	–	0.35	–
40	0.26	–	2.30
45	–	0.69	–
60	0.41	0.71	3.65
75	–	0.93	–
80	0.57	–	5.00
90	–	1.10	–
100	0.74	–	6.32
105	–	1.29	–
110	–	–	6.75
120	0.89	1.47	7.00
130	–	–	7.15
135	–	1.65	–
140	1.06	–	7.25
150	–	1.84	7.30
160	1.22	–	7.30
165	–	2.06	
180	1.41	2.26	
195	–	2.47	
200	1.58	–	
210	–	2.73	
220	1.75	–	
225	–	2.98	
240	1.91	3.14	
255	–	3.22	
260	2.09	–	
270	–	3.28	
280	2.24	–	
285	–	3.30	
300	2.34		
320	2.39		

TABLE II

Dependence of the value of factor $k_g(2)'$ on the crystallization time t_c, during crystallization of zeolite A in systems I, II, and III

t_c / min	$k_g(2)'$ / μm min^{-1} mol^{-1} dm^3		
	system I	system II	system III
10	–	–	1.43
15	–	0.61	–
20	0.37	–	1.71
30	–	0.63	–
40	0.43	–	1.93
45	–	0.60	–
60	0.47	0.65	2.00
75	–	0.67	–
80	0.48	–	2.05
90	–	0.66	–
100	0.50	–	2.08
105	–	0.66	–
110	–	–	2.06
120	0.50	0.66	1.99
130	–	–	1.93
135	–	0.66	–
140	0.51	–	1.86
150	–	0.66	1.85
160	0.52	–	1.84
165	–	0.67	
180	0.53	0.67	
195	–	0.68	
200	0.53	–	
210	–	0.70	
220	0.54	–	
225	–	0.71	
240	0.52	0.72	
255	–	0.72	
260	0.57	–	
270	–	0.724	
280	0.58	–	
285	–	0.725	
300	0.59	0.725	
320	0.60		

TABLE III

Dependence of the value of factor $k_g(3)'$ on the crystallization time t_c, during crystallization of zeolite A in systems I, II, and III

t_c / min	$k_g(3)'$ / μm^2 min^{-1} mol^{-2} dm^6		
	system I	system II	system III
10	–	–	0.023
15	–	0.076	–
20	0.035	–	0.21
30	–	0.15	–
40	0.11	–	0.61
45	–	0.23	–
60	0.19	0.30	1.02
75	–	0.39	–
80	0.26	–	1.22
90	–	0.47	–
100	0.34	–	1.88
105	–	0.54	–
110	–	–	2.05
120	0.42	0.62	2.18
130	–	–	2.27
135	–	0.70	–
140	0.50	–	2.35
150	–	0.78	2.36
160	0.58	–	2.35
165	–	0.88	–
180	0.56	0.96	2.33
195	–	1.05	–
200	0.71	–	–
210	–	1.16	–
220	0.78	–	–
225	–	1.24	
240	0.85	1.31	2.28
255	–	1.32	
260	0.91	–	
270	–	1.34	
280	0.96	–	
285	–	1.32	
300	1.00		
320	0.99		

TABLE IV

Dependence of the value of factor $k_g(4)' = k_g$ on the crystallization time t_c, during crystallization of zeolite A in systems I, II, and III

t_c / min	$k_g(4)' = k_g$ / μm min^{-1} mol^{-2} dm^6		
	system I	system II	system III
10	–	–	34.12
15	–	11.46	–
20	19.12	–	34.43
30	–	11.46	–
40	19.30	–	34.10
45	–	11.46	–
60	19.14	11.46	34.29
75	–	11.54	–
80	19.40	–	34.33
90	–	11.60	–
100	19.23	–	34.26
105	–	11.60	–
110	–	–	34.38
120	19.35	11.60	34.29
130	–	–	34.33
135	–	11.57	–
140	19.27	–	34.29
150	–	11.56	34.14
160	19.20	–	34.23
165	–	11.63	
180	19.29	11.60	
195	–	11.62	
200	19.28	–	
210	–	11.70	
220	19.28	–	
225	–	11.66	
240	19.14	11.60	
255	–	11.53	
260	19.18	–	
270	–	11.56	
280	19.19	–	
285	–	11.54	
301	19.24		
320	19.14		
average:	19.23	11.57	34.27

the kinetics of the crystal growth of zeolite A may be described by the adopted Eq. (7), *i.e.*,

$$dL_m/dt_c = k_g\,[c_{Al} - c_{Al}(eq)][c_{Si} - c_{Si}(eq)] = k_g\,f(c)_3 \qquad (16)$$

Excellent agreement between the measured values of L_m (symbols in Figure 5D) and the values of L_m calculated by Eq. (11) (curves in Figure 5D) using the average value of k_g (Table IV) and the corresponding values of I_3 (Figure 5C) confirms the relevance of Eq. (16) to the description of the kinetics of the crystal growth of zeolite A. Since Eq. (16) was derived on the basis of the Davies and Jones model of crystal growth and dissolution,[15,19] taking into consideration the particularities of zeolite crystallizing systems, it may be concluded that the growth of zeolite crystals is governed by a reaction of monomeric and/or low molecular anions from the liquid phase on the surfaces of growing zeolite crystals. Analysis of the backward reaction during the dissolution of zeolites A,[55] X,[56] and synthetic mordenite[57] in hot alkaline solutions as well as chronomal analyses of the crystal growth of silicalite-1 from clear solutions[36] has confirmed this conclusion. Also, the findings that the rates of both crystal growth[2–4,20–25,31,32] and dissolution[55–57] depend on the concentrations of both silicon and aluminium in the liquid phase is in accordance with the thesis that the growth of zeolite crystals is governed by a reaction of monomeric and/or low molecular anions from the liquid phase on the surfaces of growing zeolite crystals.[2,27–29,31,32,34,36,45,29]

CONCLUSIONS

Kinetics of the growth of zeolite A crystals crystallized under different conditions was analyzed according to different growth models. For this purpose, the concentration factors $f(c)$ (see Eqs. (2), (4), (5), and (7) relevant to different growth models) were calculated from the concentrations c_{Al} of aluminium and c_{Si} of silicon in the liquid phase of the crystallizing systems (see Figures 1B–3B), and then the $f(c)$ *vs.* t_c functions were integrated from 0 to t_c. Values of the integrals

$$I_1 = \int_0^{t_c} f(c)_1\,dt_c,\; I_2 = \int_0^{t_c} f(c)_2\,dt_c \text{ and } I_3 = \int_0^{t_c} f(c)_3\,dt_c$$

for different crystallization times t_c were used to calculate factors $k_g(1)'$, $k_g(2)'$, $k_g(3)'$, and $k_g(4)' = k_g$. Analyses of the values of the factors $k_g(1)'$, $k_g(2)'$, $k_g(3)'$, and k_g, have shown that the values of $k_g(1)'$, $k_g(2)'$, $k_g(3)'$ varied with the crystallization time t_c (see Tables I–III), thus indicating that the crystal

growth of zeolite A is neither a diffusion-controlled (see Eqs. 2 and 5) nor convection-controlled (see Eq. 4) process. This conclusion is in accordance with the findings that (i), there is no evidence for the existence of complex silicate and aluminosilicate structures in the liquid phase of crystallizing systems, and (ii) the activation energy of zeolite crystal growth is considerably higher (> 40 kJ mol^{-1}) than the activation energy (12–17 kJ mol^{-1}) that would be expected for a diffusional mechanism. On the other hand, constancy of the factor k_g during the entire process of crystallization (see Table IV) strongly indicates that the rate of crystal growth of zeolite A is proportional to the product of the fluxes of the aluminate and silicate anions, as defined by Eq. (16). In this context, it may be concluded that the crystal growth of zeolite A is governed by the reaction of monomeric and low-molecular aluminate, silicate and aluminosilicate anions from the liquid phase on the surface of growing zeolite crystals, in accordance with the Davies and Jones model for growth and dissolution, which predicts formation of a monolayer of solvated ions with a constant composition at the surface of growing/dissolving crystals. This conclusion is in agreement with results of the previous analyses of the crystal growth and dissolution of different types of zeolites.

Acknowledgement. – This work was supported by the Ministry of Science and Technology of the Republic of Croatia.

REFERENCES

1. Lj. Brečević and D. Kralj, in: N. Kallay (Ed.), *Interfacial Dynamics*, Chap. 12, Marcel Dekker Inc., New York, 1999, pp. 435–474.
2. S. Bosnar and B. Subotić, *Microporous and Mesoporous Mater.* **28** (1999) 483–493.
3. T. Antonić and B. Subotić, in: M. J. M. Treacy, B. K. Marcus, M. E. Bisher and J. B. Higgins (Eds.), *Proc. 12th Int. Conf. Zeolites*, Baltimore, MD, 1998, Material Research Society, Warrendale, PA, 1999, pp. 2049–2056.
4. S. Bosnar, J. Bronić, and B. Subotić, *Stud. Surf. Sci. Catal.* **125** (1999) 69–76.
5. A. E. Nielsen, *Croat. Chem. Acta* **42** (1970) 319–333.
6. A. E. Nielsen, *Croat. Chem. Acta* **53** (1980) 255–297.
7. P.-P. Chiang and M. D. Donohue, *AIChE Symp. Ser.* **83** (1989) 28–36.
8. J. W. Mullin, *Crystallization*, Butterworths, London, 1972, pp. 174–480.
9. A. G. Walton, *The Formation and Properties of Precipitates*, Interscience Publishers, New York-London-Sydney, 1976, pp. 44–78.
10. P. T. Cardew and R. J. Davey, *Proc. R. Soc. London, Ser. A* **398** (1985) 415–428.
11. J. Ciric, *J. Colloid Interface Sci.* **28** (1966) 315–324.
12. L. M. Truskinovskiy and E. E. Senderov, *Geokhimiya* **3** (1983) 450–461.
13. R. W. Thompson and A. Dyer, *Zeolites* **5** (1985) 202–210.
14. J. D. Cook and R. W. Thompson, *Zeolites* **8** (1988) 322–326.
15. C. W. Davies and A. L. Jones, *Trans. Faraday Soc.* **51** (1955) 812–817.
16. P. Nyvlt, *Collect. Czech. Chem. Commun.* **46** (1981) 79–85.
17. J. Budz, P. H. Karpinski, and Z. Naruc, *AIChE Symp. Ser.* **80** (1984) 89–97.

18. R. Zumstein and R. W. Rousseau, *Ind. Eng. Chem. Res.* **28** (1989) 289–297.
19. A. L. Jones and H. G. Linge, *Z. Phys. Chem. N.F.* **95** (1975) 293–296.
20. S. P. Zhdanov, in: R. F. Gould (Ed.), *Molecular Sieve Zeolites – I,* Advances in Chemistry Series, Vol. 101, American Chemical Society, Washington, DC, 1971, pp. 20–43.
21. S. P. Zhdanov and N. N. Samulevich, in: L. V. C. Rees (Ed.), *Proceedings of the Fifth International Conference on Zeolites*, Naples, 1980, Heyden, London-Philadelphia-Rheine, 1980, pp. 75–84.
22. F. Fajula, S. Nicolas, F. Di Renzo, C. Gueguen, and F Figueras, in: M. L. Occelli and H. E. Robson (Eds.), *Zeolite Synthesis*, ACS Symp. Ser. No. 398, American Chemical Society, Washington, DC, 1989, pp. 493–505.
23. B. Subotić, T. Antonić, I. Šmit, R. Aiello, F. Crea, A. Nastro, and F Testa in: M. L. Occelli and H. Kessler (Eds.), *Synthesis of Porous Materials: Zeolites, Clays and Nanostructures*, Marcel Dekker Inc., New York, 1996, pp 35–58.
24. T. Antonić, B. Subotić, and N. Stubičar, *Zeolites* **18** (1997) 291–301.
25. A. Katović, B. Subotić, I. Šmit, LJ. A. Despotović, and M. Ćurić, in: M. L. Occelli and H. E. Robson (Eds.), *Zeolite Synthesis,* ACS Symp. Ser. No. 398, American Chemical Society, Washington, DC, 1989, pp. 124–139.
26. L. S. Zevin and L. L. Zavyalova, *Kolichestvenniy Rentgenographicheskiy Prazoviy Analiz,* Nedra, Moscow, 1974, pp. 37–56.
27. R. M. Barrer, *Hydrothermal Chemistry of Zeolites*, Academic Press, London, 1982, pp. 133–182.
28. B. M. Lowe, *Stud. Surf. Sci. Catal.* **37** (1988) 1–12.
29. J. Bronić, B. Subotić, I. Šmit, and LJ. A. Despotović, *Stud. Surf. Sci. Catal.* **37** (1988) 107–114.
30. S. P. Zhdanov, N. N. Feoktitsova, and L. M. Vtjurina, *Stud. Surf. Sci. Catal.* **65** (1991) 287–296.
31. H. Kacirek and H. Lechert, *J. Phys. Chem*. **79** (1975) 1589–1593.
32. H. Kacirek and H. Lechert, *J. Phys. Chem*. **80** (1976) 1291–1296.
33. T. A. M. Twomey, M. Mackay, H. P. C. E. Kuipers, and R. W. Thompson, *Zeolites* **14** (1994) 162–168.
34. G. S. Wiersema and R. W. Thompson, *J. Mater. Chem.* **6** (1996) 1693–1699.
35. L. Gora, K. Streletzky, R. W. Thompson, and G. D. J. Phillies, *Zeolites* **18** (1997) 119–131.
36. B. J. Schoeman, J. Sterte, and J.-E. Otterstedt, *Zeolites* **14** (1994) 568–575.
37. A. E. Persson, B. J. Schoeman, J. Sterte, and J.-E. Otterstedt, *Zeolites* **15** (1995) 611–619.
38. B. J. Schoeman, J. Sterte, and J.-E. Otterstedt, *Zeolites* **14** (1994) 110–116.
39. B. J. Schoeman, J. Sterte, and J.-E. Otterstedt, *Zeolites* **14** (1994) 208–216.
40. C. S. Tsay and A. S. T. Chiang, *Microporous Mesoporous Mater.* **26** (1998) 89–99.
41. B. J. Schoeman, *Stud. Surf. Sci. Catal.* **105** (1997) 647–654.
42. A. E. Persson, B. J. Shoeman, J. Sterte, and J.-E. Otterstedt, *Zeolites* **14** (1994) 557–567.
43. P.-P. E. A. de Moor, T. P. M. Beelen, B. U. Komanschek, O. Diat, and R. A. van Santen, *J. Phys. Chem.* **B101** (1997) 11077–11086.
44. J. N. Watson, L. E. Iton, R. I. Keir, J. C. Thomas, T. L. Dovling, and J. W. White, *J. Phys. Chem.* **B101** (1997) 11094–11104.
45. C. S. Cundy, B. M. Lowe, and D. M. Sinclair, *Faraday Discuss.* **95** (1993) 235–252.
46. G. T. Kerr, *J. Phys. Chem.* **70** (1966) 1047–1050.

47. R. W. Thompson and A. Dyer, *Zeolites* **5** (1985) 202–210.
48. R. W. Thompson and A. Dyer, *Zeolites* **5** (1985) 292–301.
49. H. C. Hu, W. H. Chen, and T. Y. Lee, *J. Cryst. Growth* **108** (1991) 561–571.
50. W. H. Chen, H. C. Hu, and T. Y. Lee, *Chem. Eng. Sci.* **48** (1993) 3683–3691.
51. A. Y. Sheikh, A. G. Jones, and P. Graham, *Zeolites* **16** (1996)164–172.
52. W. Wieker and B. Fahlke, *Stud. Surf. Sci.Catal.* **24** (1985) 161–181.
53. B. Fahlke, P. Starke, V. Seefeld, W. Wieker, and K.-P. Wendlandt, *Zeolites* **7** (1987) 209–213.
54. N. Dewaele, P. Bodart, Z. Gabelica, and J. B. Nagy, *Acta Chim. Hung.* **119** (1985) 233–244.
55. A. Čižmek, LJ. Komunjer, B. Subotić, M. Široki, and S. Rončević, *Zeolites* **11** (1991) 258–264.
56. A. Čižmek, LJ. Komunjer, B. Subotić, M. Široki, and S. Rončević, *Zeolites* **11** (1991) 810–815.
57. A. Čižmek, LJ. Komunjer, B. Subotić, M. Široki, and S. Rončević, *Zeolites* **12** (1992) 190–196.

SAŽETAK

Kinetička analiza rasta kristala zeolita A

Sanja Bosnar i Boris Subotić

Promjene koncentracija, c_{Al}, aluminija i c_{Si}, silicija u tekućoj fazi kao i dimenzije najvećih kristala mjerene su tijekom kristalizacije zeolita A iz amorfnog alumosilikatnog prekursora ($Na_2O \cdot Al_2O_3 \cdot 2{,}38\ SiO_2 \cdot 1{,}66\ H_2O$) dispergiranog u lužnatim otopinama (1,2 ili 1,4 M otopina NaOH) koje sadrže (ili ne sadrže) otopljeni Al_2O_3 ili SiO_2 određene koncentracije. Analiza međuovisnosti koncentracijskih faktora $f(c) = f(c_{Al}, c_{Si})$ koji odgovaraju različitim modelima rasta i brzine rasta kristala zeolita A pokazala je da se rast kristala zeolita A odvija reakcijom monomernih i/ili niskomolekulskih aluminatnih, silikatnih i alumosilikatnih aniona iz tekuće faze na površini rastućih kristala te da se brzina rasta kristala zeolita A može izraziti kao: $dL_m/dt_c = k_g [c_{Al} - c_{Al}(eq)][c_{Si} - c_{Si}(eq)] = k_g f(c)_3$, gdje t_c je vrijeme kristalizacije, $c_{Al}(eq)$ i $c_{Si}(eq)$ su koncentracije aluminija i silicija u tekućoj fazi koje odgovaraju topljivosti zeolita A u danim uvjetima kristalizacije i k_g je konstanta linearnog rasta kristala zeolita A.